Journal of Data Acquisition and Processing
ISSN: 1004-9037
https://sjcjycl.cn/
DOI: 10.5281/zenodo.7546531

SURFACE MODIFICATION AND ANTICANCER PROPERTIES OF MXENE NANOSHEET/POLYMERS FOR BIOMEDICAL APPLICATIONS.

Mariam Ghazi A wad Alrasheedi[1*], Dr.Maged Faihan Alotaibi[2] & Prof . Nihal Saad El bialy[3]

[1*]PhD student in Medical Physics, Faculty of science king Abdul-Aziz University, Jeddah, Saudi Arabia.

[1*]Nuclear Physics lecturer, Department of Physics, College of Science and Arts, Qassim University

Qassim, Saudi Arabia. **malrasheedi0008@stu.kau.edu.sa**

[2,3]Department of Physics, Faculty of science, king Abdul-Aziz University Jeddah, Saudi Arabia.

Abstract

Here we present a facile method to produce a modified Ti_3C_2Tx from Max Phase Ti_3AlC_2 powder by etching. This process helps in controlling the characteristics and structure of MXene (MX). Then, MX was loaded with curcumin (cur) and surface modified with polyethylene glycol (PEG) forming (PEG-MXNS@cur). The physicochemical characterization of MX and PEG-MXNS@cur were investigated using several techniques, including Fourier Transform Infrared (FTIR), UV-Vis absorption spectroscopy, Zeta Sizer, Scanning Electron Microscopy (SEM), and Transmission Electron Microscopy (TEM). The results showed the successful preparation of both MX and PEG-MXNS@cur. Encapsulation efficiency of curcumin was 99%. The drug release profile showed a cumulative release rate of 53% at 24 h and 73.5% at 96 h at pH 5 and at pH 7.4, curcumin showed a release of 1.4 % at 24 h and 2.25% at 96 h. Moreover, both MX and PEG-MXNS@cur showed a cytotoxic effect on MCF7 and HepG2 cell line. PEG-MXNS@Cur showed a viability percentage of 12.89 % and 19.77 % at the concentration of 250 µg/ml which is much lower compared to Mxene alone for HepG2 and MCF7, respectively. while PEG-MXNS@cur showed IC_{50} values of 721.73 and 791.6 µg/ml for MCF7 and HepG2 cell lines, respectively. These findings suggest that PEG-MXNS@cur has the potential to be used as a therapeutic agent to treat cancer with no or little side effects. This surface modification method is also simple and easy to adopt in MXene-based research.

Keywords: Mxene, Mxene loaded curcumin, Physicochemical characterization, Cytotoxicity, Antioxidant activity.

1. Introduction

Currently, cancer is regarded as one of the world's major causes of death. Annually, more than 10 million individuals receive a diagnosis of the illness, and more than 760 million people pass away from it [1]. In terms of incidence among women worldwide, breast cancer alone is reported as the fifth leading cause of death [2].

The most conventional strategy used for cancer therapy is chemotherapy. Chemotherapy is typically administered at some point during cancer treatment. Even though chemotherapy plays a crucial role in the treatment of cancer patients, it has serious limitations in terms of therapeutic efficacy, including dose restrictions, unwanted severe side effects, and drug

resistance. Extensive research on the cellular, molecular, and genetic levels has offered a promising window into the development of alternate strategies such as nanotechnology, for battling cancer with little side effects. Nanotechnology-based cancer therapy management is one of the urgent needs for innovative, potent, and secure anticancer drugs [3–4].

MXenes are 2D carbide and nitride nanomaterials that were found in 2011. They have a high melting point, good biocompatibility, and strong metallic electrical conductivity [5–6]. Due to the abundance of surface functional groups, MXenes can be altered with a variety of substances to improve their characteristics and broaden their applicability. MXenes have more functional groups on their surface than other 2D materials, which makes modification easier. MXenes are suited for use in biomedical applications because they have entire metal atomic layers, an adjustable composition, and hydrophilicity. Additionally, MXenes may be preferable due to their efficient scale-up synthesis [6].

Despite having superior permeability and retention properties and the potential to aggregate at the tumor site, nanosized Ti_3C_2, the first MXene for drug delivery vehicles needs to be surface modified since it restacks under physiological circumstances. The modified MXenes could carry and release medicines with precision [7]. Polyethylene glycol (PEG)-treated MXene has also demonstrated encouraging results as anticancer agents and is far less harmful to normal cells [8].

The primary yellow pigment obtained from turmeric (Curcuma longa) is known as curcumin and is frequently utilized as a food flavoring agent [9]. Due to its medicinal properties in Indian and Chinese medicine, curcumin has been extensively researched for its anti-inflammatory, anti-angiogenic, antioxidant, wound-healing, and anti-cancer effects [10]. Curcumin also exhibits anti-proliferative and anti-carcinogenic characteristics in a range of cell lines and animals, according to extensive studies [11]. Additionally, recent research has demonstrated that curcumin can effectively cause apoptosis whether used alone or in conjunction with other anticancer drugs [10].

The present study aimed to surface modify MXene nanosheet with PEG (PEG-MXNS) and combine the medicinal plant curcumin for better biosafety profile. Curcumin is encapsulated with PEG-MXNS (PEG-MXNS@cur) to enhance its bioavailability and its cancer therapeutic efficacy. The current work assessed the therapeutic efficacy of PEG-MXNS@cur in comparison with free MXNS against hepatocellular carcinoma (HepG2) and breast cancer cell lines (MCF7) by measuring cytotoxicity using MTT (3-(4.5-dimrthylthiazol-2-yl)-2,5-diphenyltetrazolium bromide) assay, encapsulation efficiency, and drug release profile.

2. Materials and Methods

2.1 Materials

The basic ingredients used in the synthesis of MXene were: MAX Phase powder of Ti_3AlC_2 from (NANO SHEL. India), hydrofluoric acid from (HF, Panreac AppliChem IT Reagents) and deionized water. The pH meter was used for adjusting pH values in the experiment of Ph obtained from Sigma-Aldrich. All aqueous solutions were prepared using deionized water. Dimethyl sulfoxide (DMSO) (Merk, Darmstadt, Germany). Hepatic carcinoma (HepG2) and breast cancer (MCF7) were the two human cancer cell lines utilized in the present investigation. It has been supplied by the American Type Cell Culture Collection (ATCC, Manassas, USA) and were kept at VACSERA, Giza, Egypt. Sigma Aldrich (USA) supplied

the chemicals, namely 2,2-diphenyl-1-picrylhydrazyl (DPPH) and butylated hydroxyl toluene (BHT).

2.2 Methods

2.2.1 Fabrication of drug loaded and unloaded MXene nanoparticles.

2.2.1.1 Fabrication of MXene nanosheets (MXNSs)

Hydrofluoric acid (60 ml) was added to 3 g Ti_3AlC_2 powder stirred for 24 h at ambient temperature. Ti_3AlC_2 powder will be etched by hydrofluoric acid. 5 ml of distilled water was used to wash the reaction product. The washing was repeated several times to get rid of Al and to raise the mixture's pH above 6. Centrifugation was then used to separate the colloidal solution (Al free) Ti_3C_2Tx from the supernatant by rotating it for 30 minutes at 4000 rpm. The resulting solution of MXene was dehydrating in an oven at 80 °C for a holding time of 12 h. Finally, Mxene powder was collected for further use.

2.2.1.2 Fabrication of Polyethylene glycol -Mxene- curcumin nanosheets (PEG-MXNSs@cur)

In 25 ml of 0.1% w/v DMSO, 100 mg of Mxene was added and dissolved using magnetic stirrer. Then, 30 mg of curcumin was dissolved in 100 µl DMSO (0.1% w/v) then the volume was completed to 15 ml deionized water at 50˚C. Curcumin solution was dropwise poured to Mxene solution under magnetic stirrer (DIAHAN Scientific, Korea) for 6 h. The mixture was then incubated overnight at 37 °C in a water bath shaker for improved drug loading. Centrifuging curcumin loaded with MXene for 10 minutes at 6000 rpm separated the loaded from the unloaded curcumin... Finally, the precipitated Mxene -curcumin nanosheets were resuspended in deionized water and the formed solution was kept for further use. At the end, add 50 microliter PEG-THIO to the resuspend nanosheets, vortex and keep it in the fridge.

2.2.2 Physicochemical Characterization

2.2.2.1 FTIR spectroscopy:

The Perkin Elmer Spectrum 100 FT-IR analyzer was used to measure FTIR spectra for MXNS and PEG-MXNS@cur. Measurements were performed between the wavenumbers of 400 and 4000 cm^{-1}. The obtained results were recorded and plotted. In FTIR measurements, the samples were placed between two KBr plates to get a thin layer of the sample. These plates are then placed inside the machine and the test is started. Once the test started, IR light from the source passed through the interferometer to the specimen. The absorbance of the IR light by the aggregate takes place wherever IR beam frequency matches with that of the sample and the spectrum is recorded.

2.2.2.2 UV-VIS spectroscopy

Shimadzu (Japan) UV-Vis-NIR 3600 spectrophotometer was used for optical spectroscopic analysis. The optical properties of the samples were measured over wavelength range 200 to 800 nm. The obtained results were recorded and plotted.

2.2.2.3 Zeta Potential measurements

A zeta sizer was used to measure zeta potential values for MXNS and PEG-MXNS@cur (Zeta sizer Nano ZN, Malvern Paralytical Ltd., UK). In a disposable capillary cell, a sample is inserted to measure zeta potential value.

2.2.2.4. Scanning electron microscope (SEM)

The external features and composition of MXNS was visualized using JSM-7600F FE-SEM from JEOL, JAPAN. Energy-dispersive X-ray spectroscopy (EDX) mode has been helpful when used in conjunction with the SEM to precisely detect the elemental composition.

2.2.2.5. Transmission electron microscope (TEM)

Morphology and structure of MXNS was recorded using a high-resolution transmission electron microscope (HRTEM; Japan-made JEOL Model JEM 2100F working at 200 kV).

2.2.3 Biomedical applications

2.2.3.1 Encapsulation efficiency measurements

PEG-MXNS@cur was centrifuged at 6000 rpm for 10 min to separate the non- encapsulated drug then, the supernatant was completed to 40 ml 0.1% DMSO in water and the sample was measured in triplicate. Stock solution of curcumin in 0.1% DMSO in water with a concentration of 10 µg/ml was prepared and diluted to make a calibration curve. Finally, the samples were measured using UV-spectrophotometer (JANEWAY 6305 spectrophotometer) at wavelength = 425 nm. The encapsulation efficiency was measured using this following equation:

$$Encapsulation\ efficiency = \frac{intial\ amount\ of\ Cur - unloaded\ Cur\ in\ superntant}{intial\ amount\ of\ Cur}\ x\ 100$$

2.2.3.2 Drug release profile test

The drug release study of the prepared PEG-MXNS@cur nanosheets was conducted using dialysis bag method. Release studies were performed for samples incubated at different pH (5.5, 7.4) simulated the tumor micro-environment and normal cells, respectively [12]. Because curcumin is poorly soluble in water, release media containing 0.5% T-80 in phosphate buffered saline (pH 7.4, 5.5) was utilized. 2 ml of PEG-MXNS@cur with 0.4 mg drug was loaded into standard cellulose dialysis tubing with MWCO of 12-14 kDa. In a water bath that was shaking at 37 °C, 40 ml of release medium was added to the dialysis tube. At 1, 2, 3, 4, 5, 6, 24, 48, 72, and 96 hr, 2 ml of the dissolution medium was taken, and the fluorescence emission was recorded at excitation $\boldsymbol{\lambda}$ = 420 and emission $\boldsymbol{\lambda}$ =530. Based on a calibration curve, the total amount of released curcumin was determined, and the cumulative percentage release was calculated [13].

$$\text{Percentage Released} = \frac{\text{Mass of released curcumin}}{\text{Total Mass of curcumin}} \times 100\ \%$$

2.2.3.3 Cytotoxic study by MTT assay

The MTT (3-(4.5-dimrthylthiazol-2-yl)-2,5-diphenyltetrazolium bromide) assay was used to evaluate the cytotoxic activity of the test compounds in accordance with the published technique [14-15]. The yellow tetrazolium bromide (MTT) in this colorimetric assay is converted into a purple formazan derivative by the mitochondrial succinate dehydrogenase found in living cells. Cells were plated in 96-well plates with 10% fetal bovine serum in DMEM for 24 hours. Then, the cells were treated with MXNS and PEG-MXNS@cur (0.98, 1.95, 3.91, 7.81, 15.63, 31.25, 62.5, 125, 250, 500, 1000 and 2000 µg/ml for the MXNS) and

(0.12, 0.24, 0.49, 0.98, 1.95, 3.91, 7.81, 15.63, 31.25, 62.5, 125 and 250 µg/ml for the PEG-MXNS@cur) and incubated for 48 h. After the incubation times, the cells were subsequently treated for 2 hours with 200 µl of DMEM that contained 0.5 mg/ml of MTT. After removing the supernatant, 200 µl of DMSO were used to dissolve the formazan precipitate. The absorbance at 570 nm was then measured using a microplate reader. The relationship between cell viability % and drug concentration was plotted [16-20]. The proportion of relative cell viability was calculated as (A570 of treated samples/A570 of untreated samples) x100. The concentrations of MX and PEG-MX@cur nanosheets that inhibit 50% of cell growth were used to obtain the IC_{50} values.

3. Results and Discussion

3.1 FTIR spectroscopy

Fourier transform infrared (FTIR) spectroscopy is used for examining the physical characteristics of solids, liquids, and gases. The functional groups of both MXNS and PEG-MXNS@cur were measured using FTIR spectroscopy, Fig. 1(a) and (b).

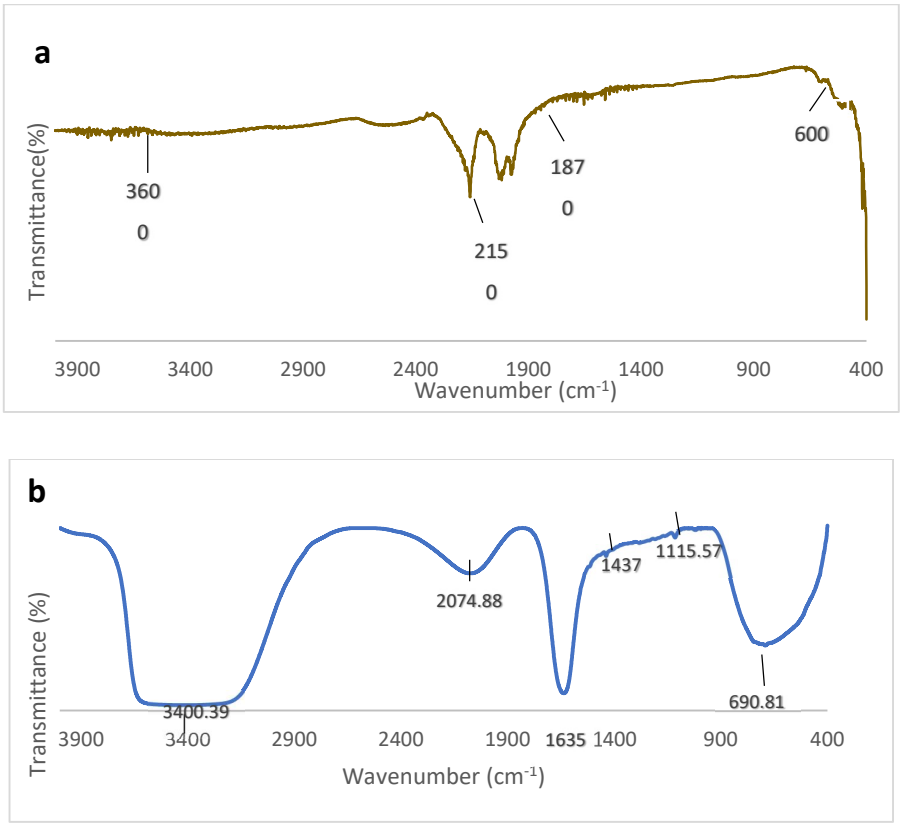

Fig. 1: FTIR spectra for (a) MXNS and (b) PEG-MXNS@cur.

In Fig. 1a, MXNS spectrum exhibited peaks between 1800 cm^{-1} to 2200 cm^{-1} corresponding to the C=O group. In addition to the presence of some peaks that could be observed between 3600 to 3900 cm^{-1}, this vibrational pattern is due to the O-H functional group [21]. Ti-O functional group is characterized by the peak at 600 cm^{-1} [22].

In Fig. 1b, PEG-MXNS@cur spectrum showed peaks at 3400 cm^{-1} and 2074 cm^{-1} that corresponds to the OH group, -C=O group, O-H group at around 1635 cm^{-1}, -OH group at

around 1437 cm^{-1}, C-F group at 1115 cm^{-1} and finally 690 cm^{-1} corresponds to Ti-O respectively [22]. In addition, it can be inferred that peaks in the range of 1600 cm^{-1} and 2100 cm^{-1} are visible in PEG-MXNS@cur spectrum, which agrees with the existence of the C=O group. A vibrational broad pattern is also seen at around 3400 cm^{-1}, which is caused by the absence of atmospheric moisture and correlates to the O-H functional set. The peak found at 690 cm^{-1} is consistent to the Ti-O functional group, and matches well with the existing literature [21-22]

3.2 UV-VIS spectroscopy

MXNS and PEG-MXNS@cur's optical response were measured using UV-VIS spectroscopy. In Fig. 2(a), MXNS spectrum showed absorption peaks at 260 nm and 700 nm because Ti_3C_2 is black in color and has a distinct absorption edge [23]. The UV-Vis absorption band's broadness is closely connected to the previously described optical properties of Mxenes; the localized surface plasma resonance (LSPR) phenomenon might be responsible for such unique attributes. Similarly, Fig. 2 (b). showed PEG-MXNS@cur absorption spectrum, although the color of the solution is blackish green and has a distinct absorption edge, nevertheless a strong optical peak can be detected over the wavelength range between 250 and 800 nm, as shown in Fig.2b. This UV-Vis absorption band's broadness is closely connected to the previously described optical properties of Mxenes and Curcumin [24-26]. The PEG-MXNS@cur exhibits a significant absorbance in between 265-300 nm region. A broad spectrum from 370- 520 nm is also observed with an associated increase in the absorption intensity compared to 435 nm for pure curcumin in DMSO [27]. Consequently, the UV-Vis bands show that the interaction combination between Mxene and curcumin was successfully formed.

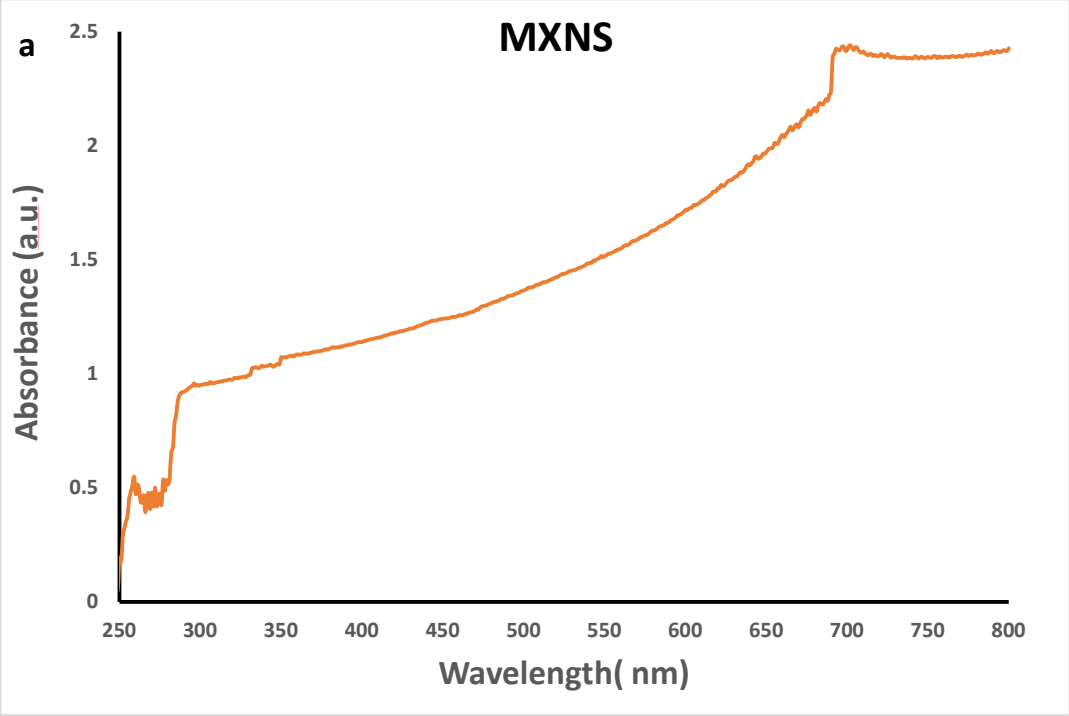

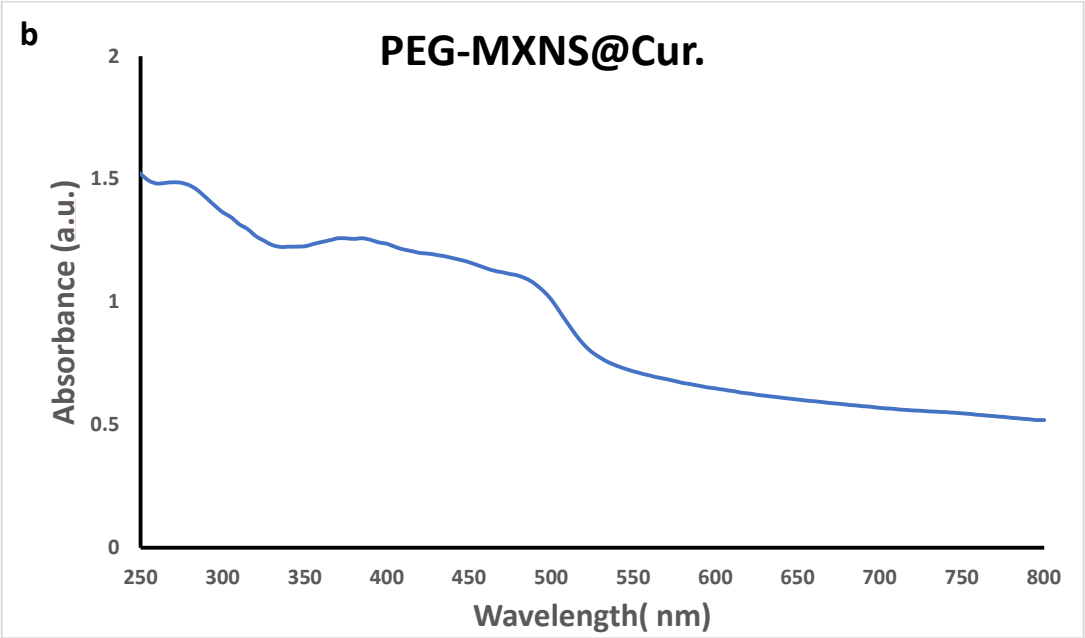

Fig. 2: UV-Vis Spectroscopy for (a) MXNS and (b) PEG-MXNS@cur.

3.3 Zeta Potential Measurements

To evaluate MXNS and PEG-MXNS@cur s' zeta potential, zeta sizer instrument has been used. The measured zeta potential values of MXNSs were -24 ± 3.85 mV, and PEG-MXNS@cur was -21.3±3.6 mV. The surface charge of MXNSs was negative which agreed with a previous study [28], but the measured zeta potential in the present study was better indicating the stability of the synthesized MXene. After curcumin loading, the negativity decreased to -21±3.6 mV [29].

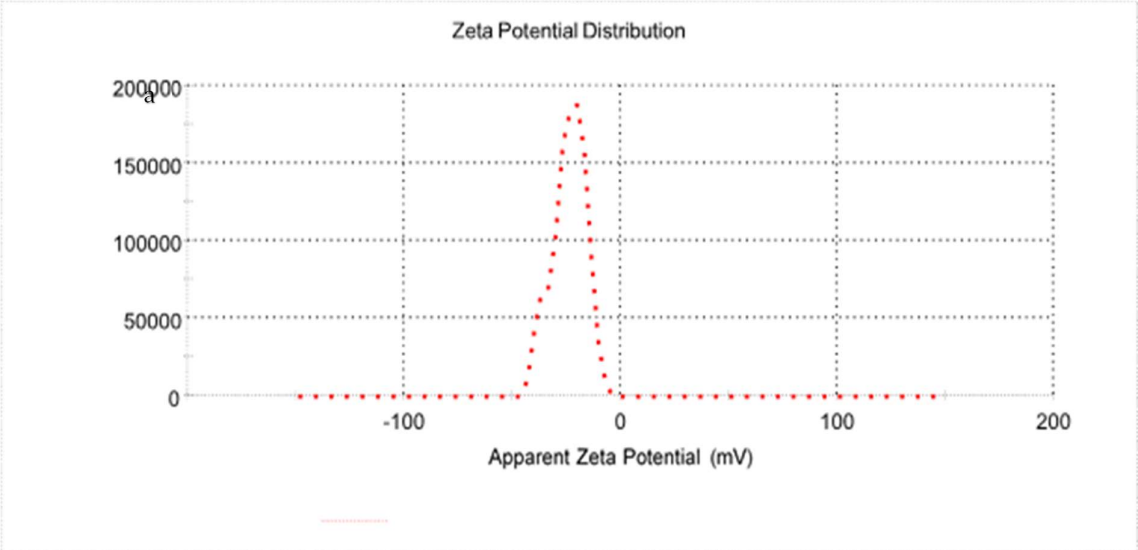

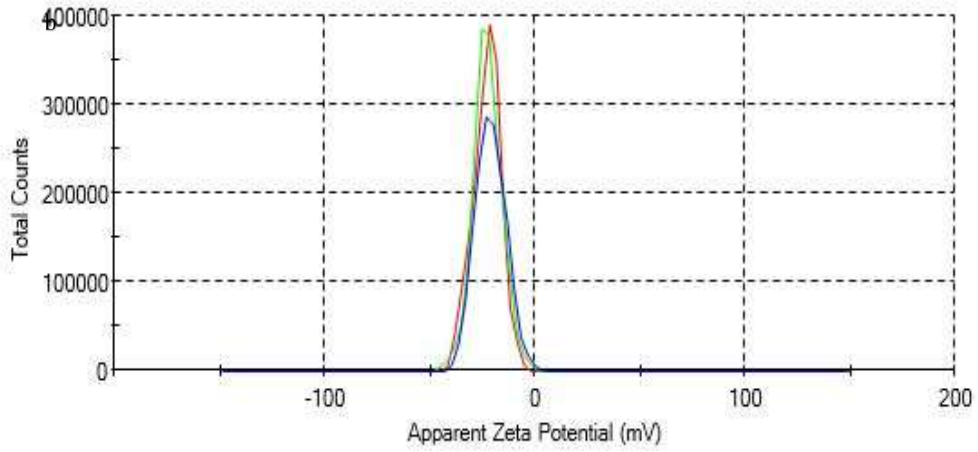

Fig. 3: Zeta Potential (a) MXNS (b) PEG-MXNS@cur.

3.4 Scanning electron microscope (SEM)

Figure 4 a, b shows that MXene was successfully exfoliated from the MAX phase once it has been etched with hydrofluoric acid (HF) solution. Since Al forms a weak metallic bond with Ti and C, Al is selectively removed during continuous HF etching of the MAX phase. The resulting MXene's have multiple stacked 2-dimensional Ti and C layers. Additionally, Mxene's composition was detected via energy dispersive spectroscopy (EDX) to be Ti, C, O, and F with minor quantities of metallic aluminum as shown in figure 4 c.

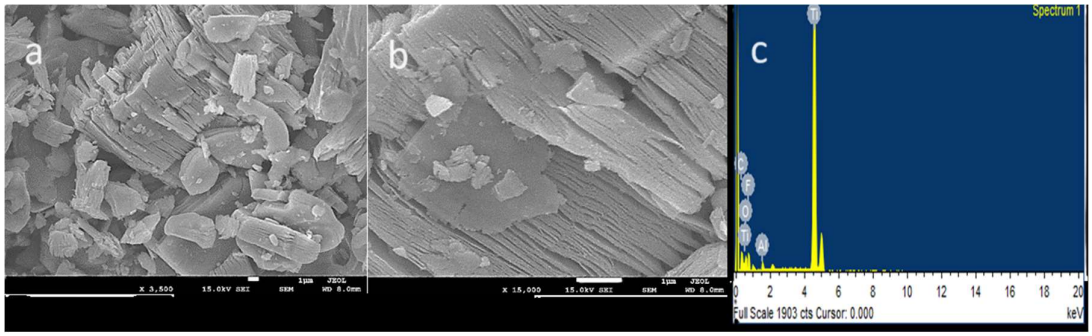

Fig. 4: SEM images (a, b) at different magnifications (c) EDX of the MXene.

And the values of the content of the elements found in the MXene are tabulated in table 1. The findings in fig. 4 indicate that the Al monolayers might be substituted by O_2 i.e., (OH) and/or fluorine. To eliminate OH and F, MXene powders can be further treated by annealing [30-34].

Table 1: Content of elements in MXene:

S. No	Element	Weight (%)	Atomic (%)
1	Titanium	70.00	44.08
2	Carbon	6.38	16.02

3	Oxygen	9.23	17.39
4	Fluorine	13.63	21.65
5	Aluminum	0.77	0.86

3.5 Transmission electron microscope (TEM)

Figure 5 demonstrates some of the acquired TEM images. The particles showed a nearly round shape and were agglomerated. High-resolution TEM images of MXene showed that the nanoparticles are between 15 and 25 nm in size, which agreed with previous studies [35-37].

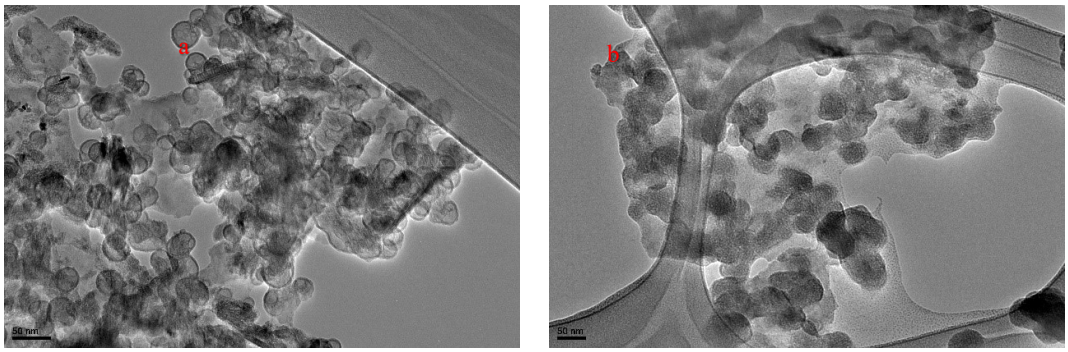

Fig. 5: TEM images of MXNS.

3.6 Encapsulation efficiency measurements

An important metric for evaluating a delivery system's encapsulation efficiency is encapsulation ability. To determine the biological activity of curcumin, the overall amount of curcumin encapsulation in PEG-MXNS@cur was evaluated. High encapsulation efficiency was demonstrated by the synthesized PEG-MXNS@cur, which reached 99 ± 0.011%. The curcumin encapsulation efficiency determined by PEG-MXNS@cur exceeded that of previous studies, suggesting that it is a dependable method of administering curcumin. [38].

3.7 Drug release profile

To evaluate the efficiency of nanosheet-based drug delivery systems in controlling drug release, an in vitro drug release profile was studied. The therapeutic efficacy of curcumin depends on its release behavior mechanism from the nanosheet-based delivery in a simulated tumor microenvironment. This is why when the nanosheets were exposed to a lower pH setting, curcumin release was observed. Curcumin loaded Mxene nanosheets were evaluated for controlled drug release in pH 5.5, 7.4. As shown in figure 6, at pH 5.5 the PEG-MXNS@cur showed quick release with a cumulative release 53% at 24 h and 73.5% at 96 h. The release of curcumin from Mxene nanosheets was observed to be at a quick rate, followed by a prolonged and sustain release. While at pH 7.4, curcumin was released slowly only about 1.4 % at 24 h and 2.25% at 96 h. Mxene nanosheets containing curcumin could achieve effective, long-term, and controlled pH-stimulated release of curcumin. The designed 2D pH responsive drug delivery system not only keeps curcumin from degrading but also sustains its release.

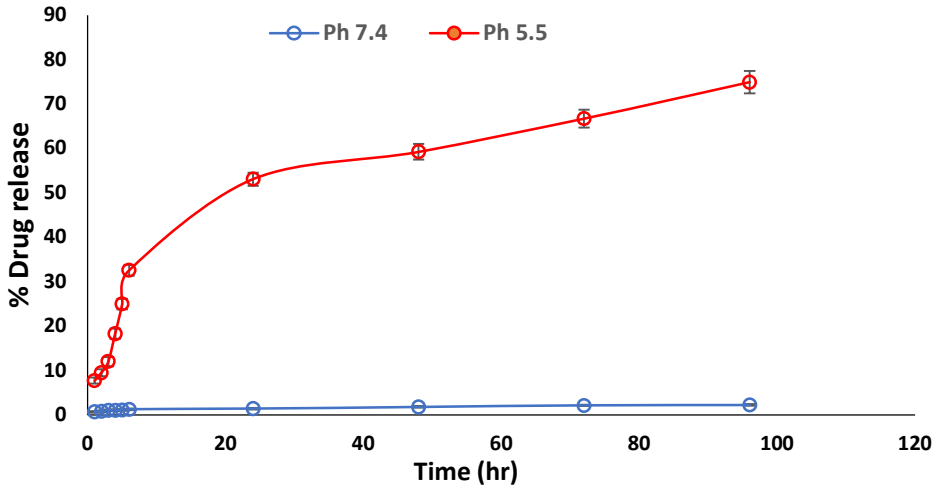

Fig.6: Curcumin release from PEG-MXNS@cur at pH 7.4 and pH 5.5 at various intervals of time.

3.8 In vitro anticancer activity

3.8.1 Cytotoxicity measurements against HepG2

The cytotoxicity of MXNS and PEG-MXNS@cur were determined using MTT assay. HepG2 cell line exposed to 0.98, 1.95, 3.91, 7.81, 15.63, 31.25, 62.5, 125, 250, 500, 1000 and 2000 µg/ml of Mxene and to 0.12, 0.24, 0.49, 0.98, 1.95, 3.91, 7.81, 15.63, 31.25, 62.5, 125 and 250 µg/ml of PEG-MXNS@cur and incubated for 48 h. Cell viability tests revealed that Mxene suppressed the growth HepG2 cell in a dose-dependent manner (Figure 7 (a)). However, Mxene caused growth inhibition of 13.26% at a very high concentration of 2000 µg/ml which indicates that Mxene has a poor anticancer ability with lower concentrations. Furthermore, the Mxene IC_{50} value was 1546 µg/ml which correlates with the poor inhibition activity for the Mxene at low concentrations (figure 7 (c)). On the other hand, the cytotoxicity of PEG-MXNS@cur showed a promising inhibition activity with lower concentrations than Mxene alone. Figure 7 (b) presents the value of PEG-MXNS@cur at maximum concentration of 250 µg/ml with a viability percentage of 12.89 % which is much lower compared to Mxene alone. These findings suggest that the conjugation of curcumin to Mxene significantly increased its anticancer properties; this is because the polyphenol present in curcumin has anticancer properties [39]. Accordingly, the IC_{50} results of the PEG-MXNS@cur was 791.6 µg/ml (figure 7 (c)) which is very much lower than Mxene alone [40].

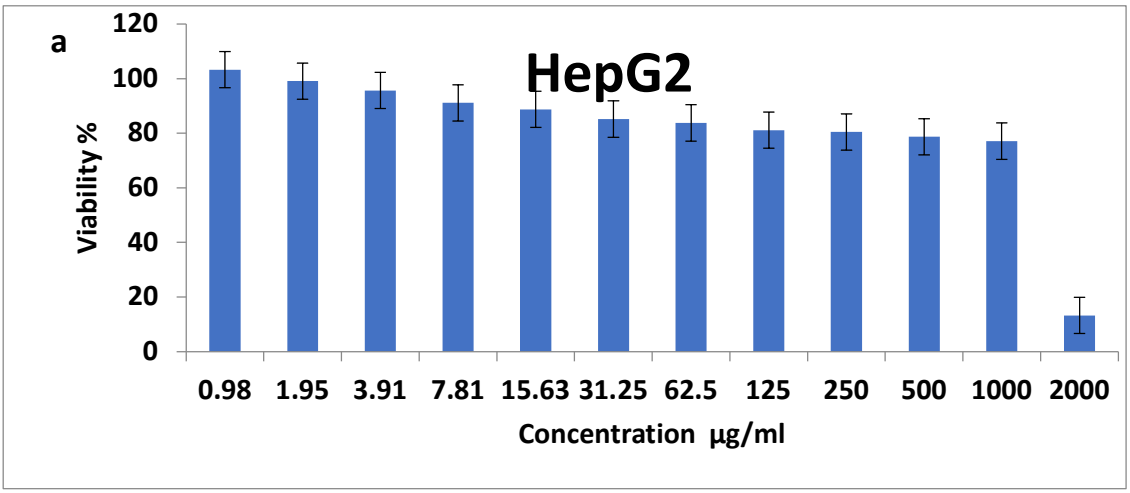

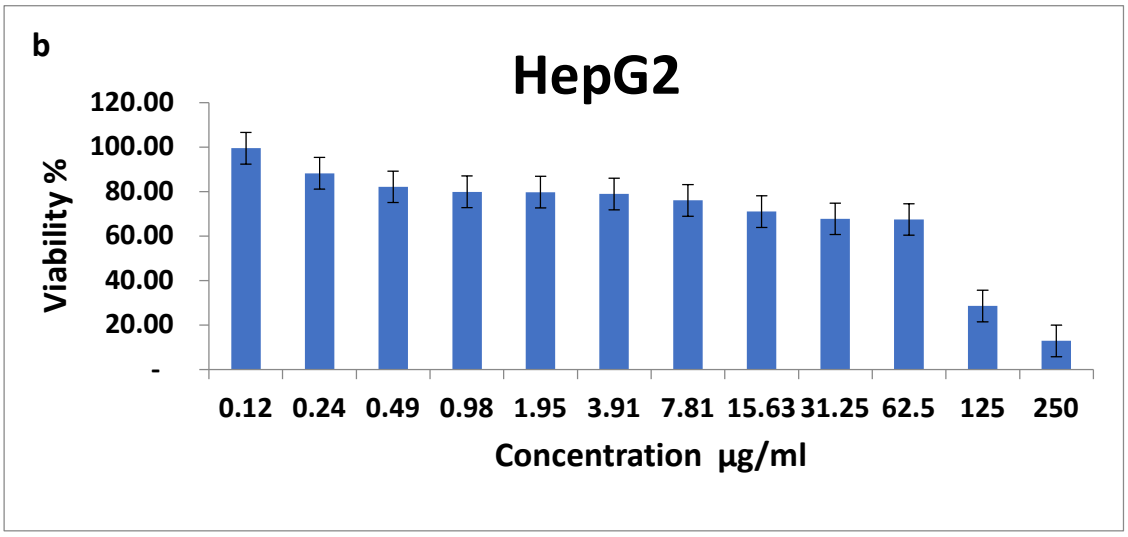

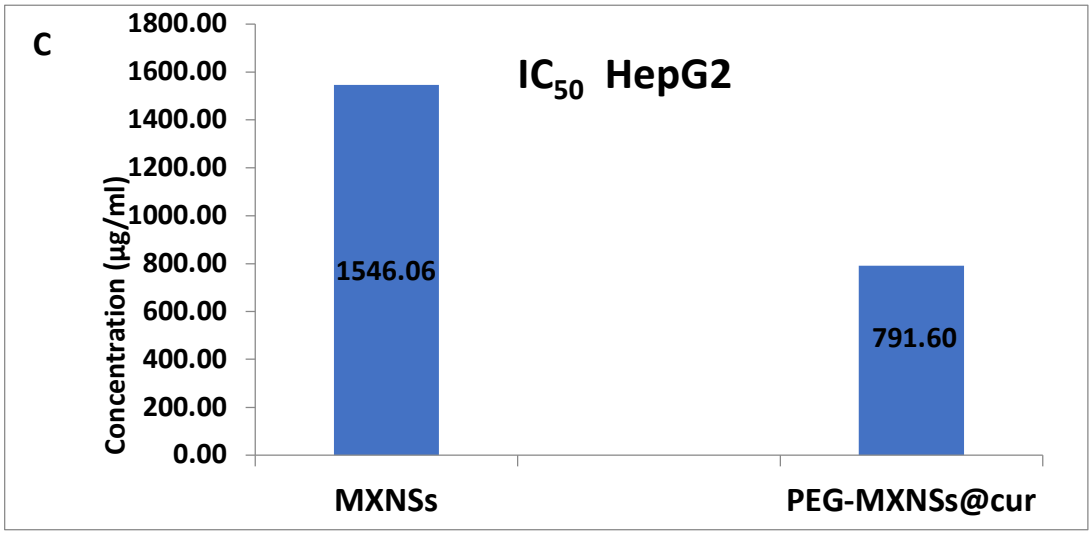

Figure 7: In-vitro study shows the effect of different concentrations of (a) MXNS, (b) PEG-MXNS@cur on the viability of HepG2 cell line after 48 h incubation time and (c) the calculated IC_{50} of the prepared nanosheets.

Figure 8 shows the micrographs of HepG2 cells treated either with MXNS or PEG-MXNS@cur with the corresponding morphological comparison with untreated control. Figure 8 (a) shows the untreated HepG2 cells with no change in morphology. Figure 8 (b) displays the cells after 48 hours of after-treatment with MXNS not being affected which correlates with the viability percentage previously mentioned. The number of cells decreased, and the remaining cells shrank in size after 48 hours of treating the cell lines with PEG-MXNS@Cur, as shown in Figure 8 (c).

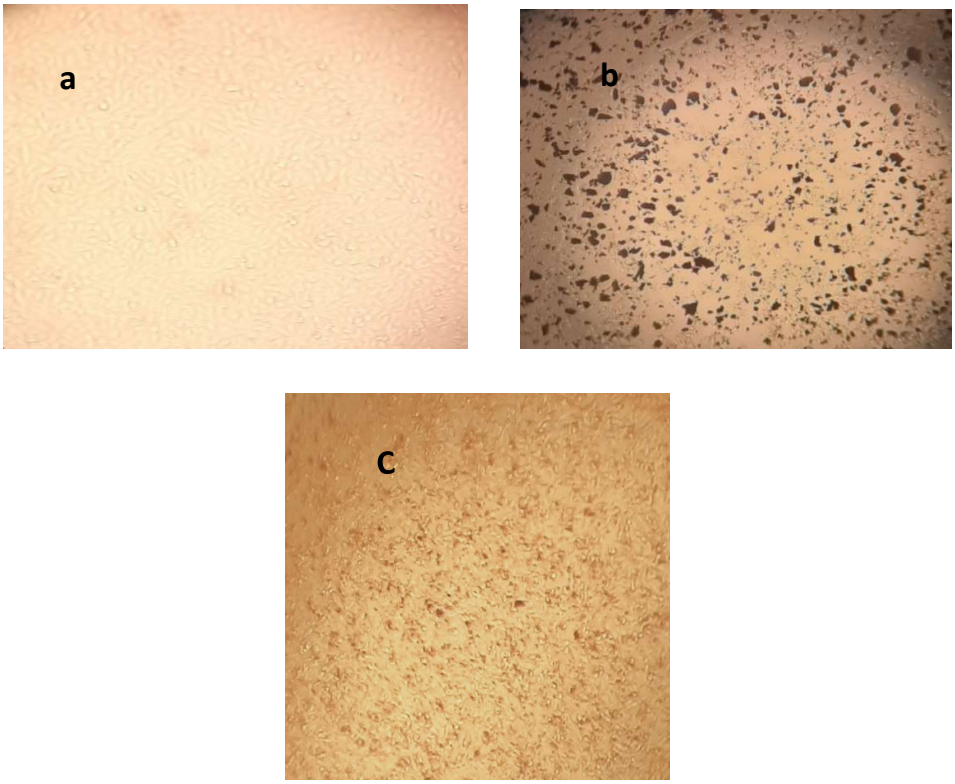

Fig.8: Photographs taken with an inverted microscope illustrate the modifications brought about by the as-prepared nanosheets (a) being the control for HepG2 cell line, (b) Mxene treated cells and (c) PEG-MXNS@cur treated cancer cells.

3.8.2 Cytotoxicity measurements against MCF7

The cytotoxicity of MXNS and PEG-MXNS@cur was determined in MCF7 cell line exposed to 0.98, 1.95, 3.91, 7.81, 15.63, 31.25, 62.5, 125, 250, 500, 1000 and 2000 µg/ml for the Mxene and to 0.12, 0.24, 0.49, 0.98, 1.95, 3.91, 7.81, 15.63, 31.25, 62.5, 125 and 250 µg/ml for the PEG-MXNS@cur at incubation time scale of 48 h. Analysis of cell viability revealed that prepared nanosheets dose-dependently inhibited the growth of the MCF7 cell line. Figure 9 (a) shows that Mxene caused inhibition of 20 % at a very ~~great~~ high concentration of 2000 µg/ml which indicates that Mxene has a poor anticancer activity against MCF-7 cell line with lower concentrations. Furthermore, the Mxene IC_{50} value was 886.5 µg/ml which correlates with the poor inhibition activity for the Mxene at low concentrations (figure 9 (c)). Figure 9 (b) illustrates the values for PEG-MXNS@cur nanosheets at the peak concentration of 250 µg/ml with a viability percentage of 19.77 % which is very much lower compared to Mxene alone.

These findings show that curcumin loading in Mxene significantly increased its growth inhibitory effects on breast cancer cells. This is attributed to DNA alteration caused by oxidative stress brought on by curcumin through the generation of ROS and oxidative damage [41]. Accordingly, the IC_{50} results of the PEG-MXNS@cur was 721.22 µg/ml (figure 9 (c)) which is very much lower than Mxene alone indicating a better cancer growth inhibition property than Mxene.

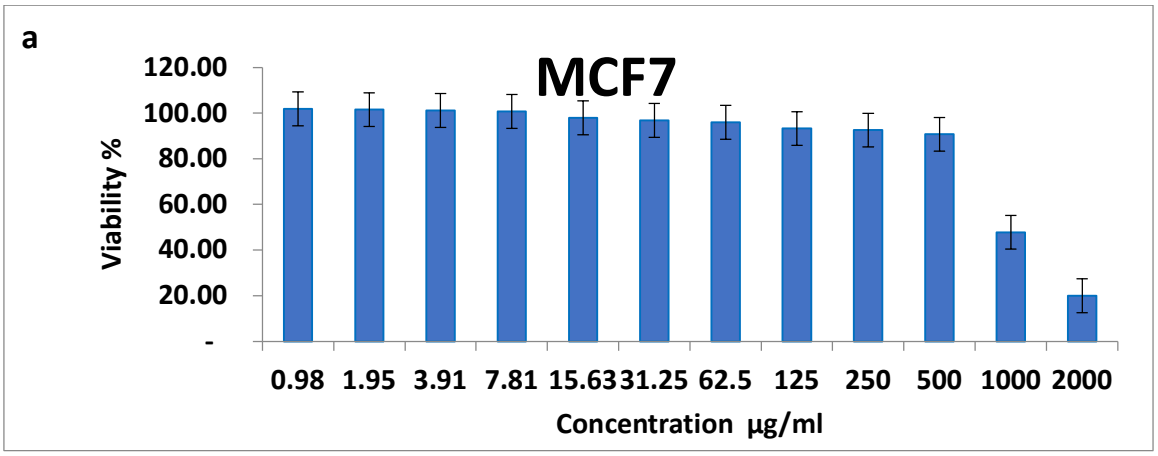

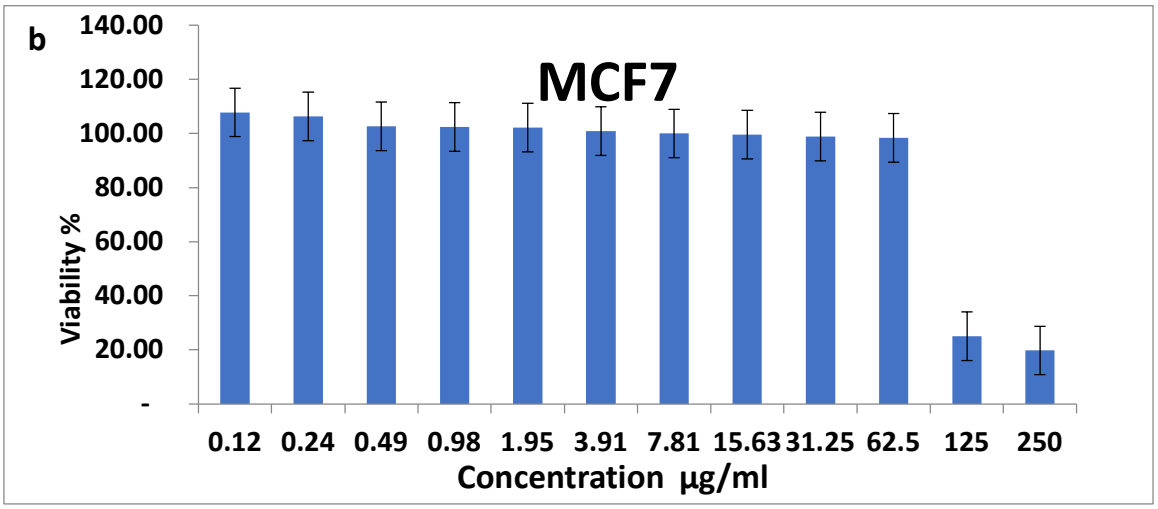

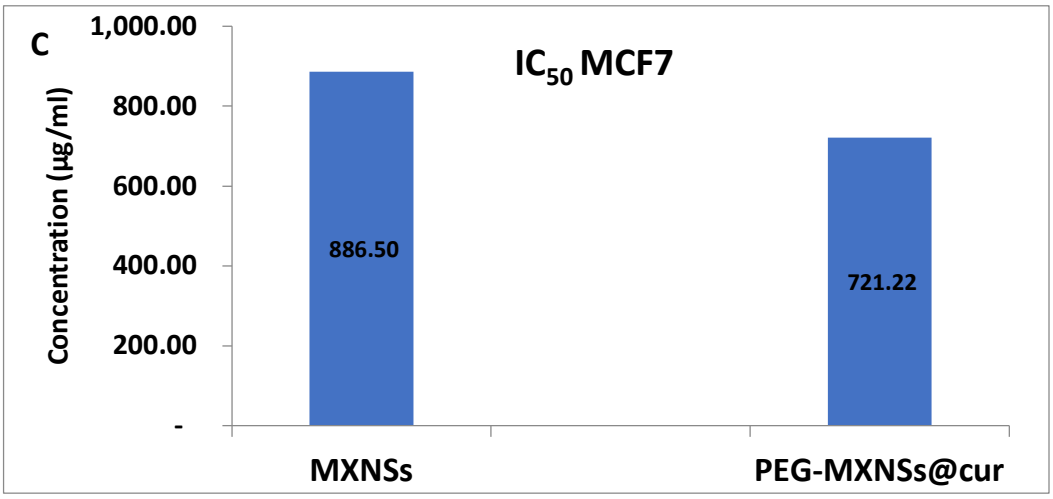

Figure 9: In-vitro study reveals the effect of various concentrations of (a) MXNS, (b) PEG-MXNS@cur on the viability of MCF7 cell line after 48 h and (c) the calculated IC_{50} of the prepared nanosheets.

Figure 10 displays micrographs of the MCF7 cells treated with MXNS and PEG-MXNS@cur in comparison with untreated control. Figure 10 (b) shows MCF-7 cells after being exposed to ~~s~~ Mxene dose (125 µg/ml) for 48 hours are unaffected to some extent and are consistent with the previously indicated viability percentage. Figure 10 (c) the PEG-MXNS@Cur treated cells, however, shows apoptotic cell after 48 hours. It is worthy noted that the of PEG-MXNS@cur showed better therapeutic efficacy against MCF-7 over HepG2 cells. Figure 10 (a) shows untreated cells (negative control group) with its normal morphological shape.

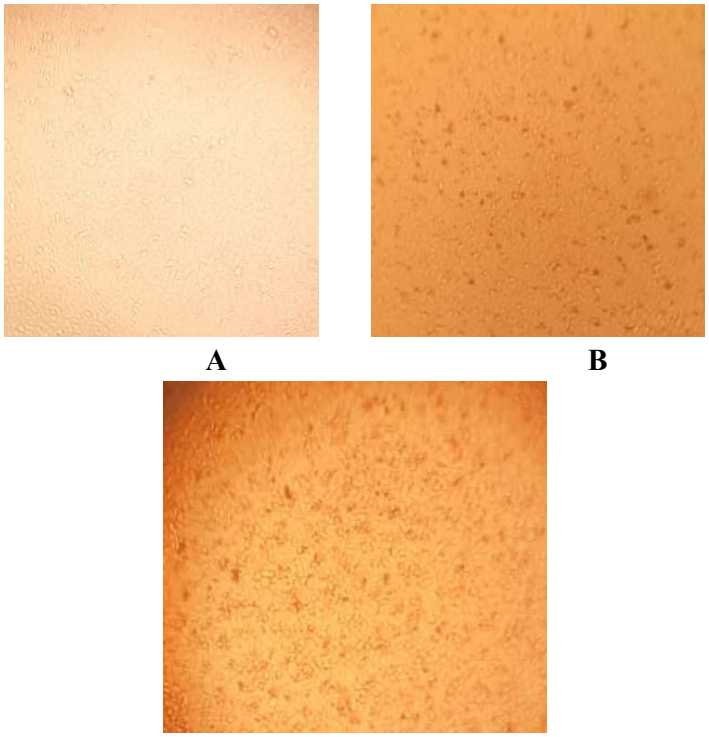

Figure 10: Inverted microscope photographs of MCF7- cells line: (a) untreated, (b) treated with MXNS and (c) treated with PEG-MXNS@cur.

4. Conclusion

1. Modified Ultrathin-MXene was successfully synthesized and characterized for biomedical applications using a facile selective etching process.
2. The Modified Ultrathin-MXene was loaded with Curcumin to study its anticancer properties.
3. The Mxene loaded Curcumin exhibited good acceptance of Curcumin in the Mxene solution supported by the zeta potential values.
4. The prepared nanosheets exhibited a good encapsulation efficiency of 99 ± 0.011%.

References

1. Bray F, Ferlay J, Soerjomataram I, Siegel RL, Torre LA, Jemal A. Global cancer statistics 2018: GLOBOCAN estimates of incidence and mortality worldwide for 36 cancers in 185 countries. CA Cancer J Clin. 2018;68(6):394-424.
2. Thoidingjam S, Tiku AB. New developments in breast cancer therapy: role of iron oxide nanoparticles. Advances in Natural Sciences: Nanoscience and Nanotechnology. 2017;8(2):023002
3. Darwesh, R., & Elbialy, N. S. (2021). Iron oxide nanoparticles conjugated curcumin to promote high therapeutic efficacy of curcumin against hepatocellular carcinoma. Inorganic Chemistry Communications, 126, 108482.
4. N. Amanlou, M. Parsa, K. Rostamizadeh, S. Sadighian, F. Moghaddam, enhanced cytotoxic activity of curcumin on cancer cell lines by incorporating into gold/ chitosan nanogels, Mater. Chem. Phys. 226 (2019) 151–157.
5. Naguib, M.; Kurtoglu, M.; Presser, V.; Lu, J.; Niu, J.; Heon, M.; Hultman, L.; Gogotsi, Y.; Barsoum, M.W. (2011). "Two-Dimensional Nanocrystals Produced by Exfoliation of Ti3AlC2". Advanced Materials. 23 (37): 4248–4253.
6. Naguib, M.; Mochalin, V.N.; Barsoum, M.W.; Gogotsi, Y. (2011). "25th Anniversary Article: MXenes: A New Family of Two-Dimensional Materials". Advanced Materials. 26 (7): 992–1005
7. Huang, J., Li, Z., Mao, Y., & Li, Z. (2021). Progress and biomedical applications of MXenes. *Nano Select*, *2*(8), 1480-1508.
8. Lin, H.; Wang, X.; Yu, L.; Chen, Y.; Shi, J. Two-Dimensional Ultrathin MXene Ceramic Nanosheets for Photothermal Conversion. Nano Lett. 2017, 17, 384–391.
9. Kizhakkayil J, Thayyullathil F, Chathoth S, Hago A, Patel M, Galadari S. Modulation of curcumin-induced Akt phosphorylation and apoptosis by PI3K inhibitor in MCF-7 cells. *Biochem Biophys Res Commun.* 2010;**394**(3):476–81.
10. Lv ZD, Liu XP, Zhao WJ, Dong Q, Li FN, Wang HB, et al. Curcumin induces apoptosis in breast cancer cells and inhibits tumor growth in vitro and in vivo. Int J Clin Exp Pathol. 2014;7(6):2818–24.
11. Chen CC, Sureshbabul M, Chen HW, Lin YS, Lee JY, Hong QS, et al. Curcumin Suppresses Metastasis via Sp-1, FAK Inhibition, and E-Cadherin Upregulation in Colorectal Cancer. Evid Based Complement Alternat Med. 2013; 2013:541695.

12. Tang, R.; Zhou, S.; Li, C.; Chen, R.; Zhang, L.; Zhang, Z.; Yin, L. Janus-Structured Co-Ti3C2 MXene Quantum Dots as a Schottky Catalyst for High-Performance Photoelectrochemical Water Oxidation. Adv. Funct. Mater. 2020, 30, 2000637.
13. Luo, Q.; Chai, B.; Xu, M.; Cai, Q. Preparation, and photocatalytic activity of TiO2-loaded Ti3C2 with small interlayer spacing. Appl. Phys. A 2018, 124, 495. [CrossRef]
14. W. Chen, J. Ouyang, X. Yi, Y. Xu, C. Niu, W. Zhang, L. Wang, J. Sheng, L. Deng, Y. N. Liu and S. Guo, Adv. Mater., 2018, 30, 1703458–1703464.
15. X. Ren, M. Huo, M. Wang, H. Lin, X. Zhang, J. Yin, Y. Chen and H. Chen, ACS Nano, 2019, 13, 6438–6454.
16. Z. Wang, K. Yi, Q. Lin, L. Yang, X. Chen, H. Chen, Y. Liu and D. Wei, Nat. Commun., 2019, 10, 1544–1553.
17. C. Zheng, X. Jin, Y. Li, J. Mei, Y. Sun, M. Xiao, H. Zhang, Z. Zhang and G. J. Zhang, Sci. Rep., 2019, 9, 759–767.
18. Zamhuri, A.; Lim, G. P.; Ma, N. L.; Tee, K. S.; Soon, C. F. J. B. e. o. MXene in the lens of biomedical engineering: synthesis, applications, and outlook. Biomedical engineering online 2021, 20, 33, DOI: 10.1186/s12938-021-00873-9.
19. Philoppes, J. N., & Lamie, P. F. (2019). Design and synthesis of new benzoxazole/benzothiazole-phthalimide hybrids as antitumor-apoptotic agents. Bioorganic chemistry, 89, 102978.
20. J.M. Edmondson, L.S.Armstrong, A.O. Martinez, Manual of microbiologic monitoring of laboratory animals,J. Tiss. Cult.Meth.11(1988), 5.
21. Tang, Q.; Zhao, Y.; Du, X.; Chong, L.; Gong, P.; Guo, C. Design, Synthesis, and Structure- Activity Relationships of Novel 6,7-Disubstituted-4-Phenoxyquinoline Derivatives as Potential Antitumor Agents. Eur. J. Med. Chem. 2013, 69, 77–89.
22. Youssif, B. G. M.; Abdelrahman, M. H.; Abdelazeem, A. H.; Abdelgawad, M. A.; Ibrahim, H. M.; Salem, O. I. A.; Mohamed, M. F. A.; Treambleau, L.; Nasir, S.; Bukhari, A. Design, Synthesis, Mechanistic and Histopathological Studies of Small-Molecules of Novel Indole- 2-Carboxamides and Pyrazino [1,2-a]Indol-1(2H)-Ones as Potential Anticancer Agents Effecting the Reactive Oxygen Species Production. Eur. J. Med. Chem. 2018, 146, 260–273.
23. A. Sudha, J. Jayachandran, P. Srinivasan, Green synthesis of silver nanoparticles using Lippianodiflora aerial extract and evaluation of their antioxidant.
24. Teixeira, P. V., Adega, F., Martins-Lopes, P., Machado, R., Lopes, C. M., & Lúcio, M. (2023). pH-Responsive Hybrid Nanoassemblies for Cancer Treatment: Formulation Development, Optimization, and In Vitro Therapeutic Performance. Pharmaceutics, 15(2), 326.
25. Yunfei Huang, Yiling Zhan, Guangyi Luo, Yan Zeng, David Julian McClements, Kun Hu, Curcumin encapsulated zein/caseinate-alginate nanoparticles: Release and antioxidant activity under in vitro simulated gastrointestinal digestion, Current Research in Food Science, Volume 6, 2023, 100463, ISSN 2665-9271, https://doi.org/10.1016/j.crfs.2023.100463.
26. Satheeshkumar, E., Makaryan, T., Melikyan, A. et al. One-step Solution Processing of Ag, Au, and Pd@MXene Hybrids for SERS. Sci Rep 6, 32049 (2016).
27. Q. Xue, H. Zhang, M. Zhu, Z. Pei, H. Li, Z. Wang, Y. Huang, Y. Huang, Q. Deng, J. Zhou, S. Du, Q. Huang and C. Zhi, Adv., Mater., 2017, 29, 1604847.

28. Xie, Y.; Rahman, M.M.; Kareem, S.; Dong, H.; Qiao, F.; Xiong, W.; Liu, X.; Li, N.; Zhao, X. Facile synthesis of CuS/MXene nanocomposites for efficient photocatalytic hydrogen generation. CrystEngComm 2020, 22, 2060–2066.
29. Tang, R.; Zhou, S.; Li, C.; Chen, R.; Zhang, L.; Zhang, Z.; Yin, L. Janus-Structured Co-Ti3C2 MXene Quantum Dots as a Schottky Catalyst for High-Performance Photoelectrochemical Water Oxidation. Adv. Funct. Mater. 2020, 30, 2000637.
30. Luo, Q.; Chai, B.; Xu, M.; Cai, Q. Preparation, and photocatalytic activity of TiO2-loaded Ti3C2 with small interlayer spacing. Appl. Phys. A 2018, 124, 495. [CrossRef]
31. Xuan, J.; Wang, Z.; Chen, Y.; Liang, D.; Cheng, L.; Yang, X.; Liu, Z.; Ma, R.; Sasaki, T.; Geng, T. Organic-base-driven intercalation and delamination to produce functionalized titanium carbide nanosheets with superior photothermal therapeutic performance. Angew. Chem. 2016, 128, 14789–14794. [CrossRef].
32. Subhan, M. A., Alam, K., Rahaman, M. S., Rahman, M. A., & Awal, R. (2013). Synthesis and Characterization of Metal Complexes Containing Curcumin (C₂₁H₂₀O₆) and Study of their Anti-microbial Activities and DNA-binding Properties. Journal of Scientific Research,2014, 6(1), 97–109.
33. A. M. Jastrzębska, E. Karwowska, P. Kurtycz, A. R. Olszyna, A. Kunicki, Surf. Coat. Technol.2015. 271.
34. A. M. Jastrzębska, J. Jureczko, A. R. Kunicki, A. R. Olszyna, Int. J. Appl. Ceram. Technol. 2015. 12.
35. A. M. Jastrzębska, J. Jureczko, A. R. Kunicki, A. R. Olszyna, Int. J. Appl. Ceram. Technol. 2015. 12.
36. Kang, R., Zhang, Z., Guo, L. et al. Enhanced Thermal Conductivity of Epoxy Composites Filled with 2D Transition Metal Carbides (MXenes) with Ultralow Loading. Sci Rep 9, 9135 (2019).
37. Naguib M, Kurtoglu M, Presser V, Lu J, Niu J, Heon M, Hultman L, Gogotsi Y, Barsoum MW. Two-dimensional nanocrystals produced by exfoliation of Ti3 AlC2. Adv Mater. 2011 Oct 4;23(37):4248-53.
38. Sari, T. P., Mann, B., Kumar, R., Singh, R. R. B., Sharma, R., Bhardwaj, M., & Athira, S. (2015). Preparation and characterization of nanoemulsion encapsulating curcumin. *Food Hydrocolloids*, *43*, 540-546.
39. Naguib M, Kurtoglu M, Presser V, Lu J, Niu J, Heon M, Hultman L, Gogotsi Y, Barsoum MW. Two-dimensional nanocrystals produced by exfoliation of Ti3 AlC2. Adv Mater. 2011 Oct 4;23(37):4248-53.
40. Zhang J, Li S, Hu S, Zhou Y. Chemical Stability of Ti_3C_2 MXene with Al in the Temperature Range 500-700 °C. Materials (Basel). 2018 Oct 15;11(10):1979.
41. Kumar, R., Maji, B. C., & Krishnan, M. (2020). Synthesis of 2D material MXene from Ti3AlC2 MAX-phase for electromagnetic shielding applications. DAE SOLID STATE PHYSICS SYMPOSIUM 2019.